INTERNATIONAL JOURNAL OF REMOTE SENSING
https://doi.org/10.1080/01431161.2019.1708506

Taylor & Francis
Taylor & Francis Group



# A dielectric model of thawed and frozen Arctic soils considering frequency, temperature, texture and dry density

V. L. Mironov[a], A. Yu. Karavayskiy[a], Yu. I. Lukin[a] and I. P. Molostov[b]

[a]Kirensky Institute of Physics, Federal Research Center KSC SB RAS, Krasnoyarsk, Russia; [b]Altai State University, Barnaul, Russia

**ABSTRACT**

A dielectric model was developed for thawed and frozen mineral soils, based on the refractive mixing dielectric formula and the dielectric measurement data for three soils collected in the Arctic tundra of the Yamal Peninsula. The refractive mixing dielectric model was used in conjunction with the Debye multi relaxation equations as a theoretical model to fit the measured complex relative permittivity spectra as a function of soil moisture and temperature. As a result, the dielectric spectroscopic parameters for the various components of water in the soil, such as the low- and high-frequency limits of the complex relative permittivity, the times of the corresponding relaxations, and the specific conductivity, were simultaneously determined for soils with different clay contents for all measured temperatures. As the theoretical temperature dependences of these parameters, the Clausius–Mossotti, Eyring, and linear equations for the conductivity were used. By using approximations of the measured data with these formulas, the parameters of the temperature-dependent model were derived, such as the coefficient of volume expansion, energy and entropy of activation, and coefficient of thermal conductivity. A set of the parameters discussed above in conjunction with the refractive mixing formula is a temperature- and mineralogically dependent multi-relaxation spectroscopic dielectric model, which enables estimation of the permittivity of moist soils as a function of dry soil density, moisture, frequency, temperature, and texture. The statistical error of the proposed dielectric model was estimated in terms of the normalized root-mean-square error (nRMSE), which was equal to 5% and 25% for the dielectric constant and dielectric loss factor, respectively.

**ARTICLE HISTORY**
Received 15 July 2019
Accepted 28 October 2019

## 1. Introduction

The development of dielectric models of moist soils of the top layers of the Earth is an important part of creating remote-sensing algorithms for the land surface. The fact that this dielectric models used in remote-sensing algorithms establish the relationship between the radiation of radio and radar scattering soil surface with geophysical parameters.

**CONTACT** A. Yu. Karavayskiy rsdak@ksc.krasn.ru Kirensky Institute of Physics, Federal Research Center KSC SB RAS, 660036 Krasnoyarsk, Russia

At present, different satellite systems use individual dielectric models to retrieve the moisture profile. For example, in the algorithms the Airborne Microwave Observatory of Subcanopy and Subsurface (AIRMOSS) platform (Tabatabaeenejad et al. 2014) based on P-band the dielectric model developed in Peplinski, Ulaby, and Dobson (1995) is used. In the L-band, remote-sensing algorithms for satellite systems Soil Moisture and Ocean Salinity (SMOS) and Soil Moisture Active Passive (SMAP) (Mialon et al. 2015; Wigneron et al. 2017; Zeng et al. 2016) used the dielectric model proposed in articles (Mironov et al. 2004; Mironov, Kosolapova, and Fomin 2009). In the X-band, the models (Wang and Schmugge 1980; Dobson et al. 1985) were used in soil moisture retrieval algorithms based on radiometric data from Advanced Microwave Scanning Radiometer – Earth Observing System (AMSR-E) (Jackson et al. 2010) and Global Change Observation Mission – Water (GCOM-W1) (Bindlish et al. 2017). Each of these satellite systems uses its own dielectric model. In order to process remote-sensing data obtained simultaneously from several satellite systems, certain difficulties arise associated with a variety of dielectric models. Satellite systems in a wide frequency range (MHz and GHz ranges) require the development of an appropriate general dielectric model, which is the first step on the path of wideband remote sensing.

In relation to the problems of remote sensing, a number of dielectric models have been developed and are applied. The first dielectric model at various frequencies, for soils with different textures at a fixed positive temperature, was proposed by Wang and Schmugge (1980). This model is based on a mixture model. Where the components of the mixture are mineral particles, air and water. In this case, the presence of two components of water in soil was postulated, called bound water, which is adsorbed on the surface of mineral particles and free water, which is contained in the capillaries of the soil. In developing this model, the values of the real and imaginary parts of the complex relative permittivity (CRP) of free water were experimentally measured for water outside the soil at a temperature of 20 °C; for example, at a frequency of 1.4 GHz, values of 79.5 and 6.63 were used, respectively. For mineral particles, experimental CRP values were also used. The main novelty of this model was that it allowed the dependence of the CRP of moist soil on its texture to be expressed at fixed values of wave frequency.

Later, a spectroscopic dielectric model was proposed by Dobson et al. (1985) for the CRP of moist soils in the frequency range from 1.4 to 18 GHz, which is the most widely quoted in the literature. This model, as well as that suggested by Wang and Schmugge (1980) was based on a mixture formula. The composition of the mixture included the same soil components as the model by Wang and Schmugge (1980), but Dobson et al. (1985) assumed that the CRP spectra of water in soil coincide with the CRP spectra of water outside the soil. To describe these spectra at a fixed temperature, the Debye equation, which was modified to account for the dielectric losses caused by conductivity of the soil water, was applied. The effect of bound water was considered by introducing the value of reduced moisture, which depends on the soil texture. The exponent of the mixture model and the effective amount of water for each of the measured soils were determined by Dobson et al. (1985) by best fitting the used theoretical model to the respective measured soil dielectric data. According to Dobson et al. (1985), the model describes the measured data well in the frequency range from 4 to 18 GHz at a fixed positive temperature of 20 °C.

The spectroscopic dielectric model, which would significantly reduce the error of predicting CRP moist soil in a wider frequency band, was later proposed by Mironov, Kosolapova, and Fomin (2009). As in Wang and Schmugge (1980) and Dobson et al. (1985), this dielectric model is based on a mixture model, written by analogy with Dobson et al. (1985) in a certain frequency range. The essential difference between the dielectric model proposed by Mironov, Kosolapova, and Fomin (2009) from the models proposed by Dobson et al. (1985) is that the refractive equation mixture is applied Birchak et al. (1974), which is recorded for the complex refractive index of the mixture and its components, namely, mineral particles, bound water, free water, and air. In this case, to describe the CRP spectra of both bound and free water, the corresponding Debye equations were modified to account for the dielectric losses caused by conductivity of the soil water. The relative content of bound water and the parameters of these equations, namely the static dielectric constant and relaxation time of bound and free water, were determined by fitting the measured experimental CRP spectra of individual moist soils (having fixed clay content), which achieved the best fit of the experimental data and theoretical values. As a result, dependences of the parameters of the spectroscopic model on the content of the clay fraction at a fixed temperature were obtained. The proposed model in the literature received the name of the generalized refractive mixture dielectric model (GRMDM). This approach has significantly reduced the error in determining the CRP values of moist soils, compared with the model (Dobson et al. 1985) in the frequency range from 1.4 to 4 GHz, and expands the range of application of the spectroscopic model of the moist soil to frequencies as low as 0.3 GHz.

Later in Mironov and Fomin (2009a) a spectroscopic dielectric model of thawed moist soil was created that considers the temperature dependence with a fixed texture. As a first step in constructing this model, GRMDM was used for soil with a fixed particle size distribution at a given set of temperatures. As a result, the experimental dependences on the temperature of the static dielectric constant and relaxation times for bound and free water in the soil were determined. For the theoretical temperature dependences of these parameters, Clausius–Mossotti, Eyring and conductivity formulas were applied. The parameters proposed by Mironov and Fomin (2009a) for the temperature-dependent spectroscopic model were determined by the best fit between the experimental values and the values calculated using theoretical formulas. The parameters that depend on temperature are the static dielectric constant at the initial temperature, volume-expansion coefficients, entropy of activation, activation energy of the relaxation process, and specific conductivity of the components of bound and free water in the soil. This model is called the temperature dependent generalized refractive mixing dielectric model (TD GRMDM).

Because changes in both temperature and soil texture are observed under natural conditions, it became necessary to create dielectric models of moist soils that consider the influence of both these factors. Such a dielectric model was proposed by Mironov and Fomin (2009b). TD GRMDM was used as an initial model, which was applied to each of the experimental spectra obtained for a set of soils with a different texture and measured in the temperature range from 10 to 40 °C (Curtis, Weiss, and Everett 1995). The experimental dependences of the TD GRMDM parameters obtained for different measured soils were approximated by a set of polynomial formulas as a function of clay content. As a result, a dielectric model was proposed to describe the CRP of moist soils as a function of moisture, frequency, temperature, and clay content. Such a model is called the temperature- and mineralogy-dependent soil dielectric model (TMD SDM).

It should be noted that the models developed earlier described the experimental CRP spectra of moist soils for frequencies above 300 MHz. The use of these models to describe CRP spectra below 300 MHz was not possible due to a significant increase in model errors in this frequency range. This is because Debye's single-relaxation model, used in Mironov, Kosolapova, and Fomin (2009) and Mironov and Fomin (2009a, 2009b) does not account for the significant increase in the real and imaginary parts of the CRP of moist soils with decreasing frequency observed in experiments (Dobson et al. 1985; Curtis, Weiss, and Everett 1995; Wagner et al. 2011). In this regard, based on the approach (Mironov, Bobrov, and Fomin 2013a, 2013b; Mironov et al. 2013a) for the creation of GRMDM, proposed introducing additional dielectric relaxations for the soil water components into the Debye spectroscopic low-frequency region. This allowed the proposed multi-relaxation dielectric model of the CRP spectra of the moist soil in the frequency range from 40 MHz to 300 MHz to achieve the same errors as observed for the previously developed single-relaxation dielectric models in the frequency range above 300 MHz (Mironov, Kosolapova, and Fomin 2009; Mironov and Fomin 2009a, 2009b). The proposed model was called the multi-relaxation generalized refractive mixing dielectric model (MR GRMDM).

All the models discussed above were obtained for soils at a positive temperature. A significant difference in the state of moist soil at a negative temperature is that part of the water may be in a state of ice, if the moisture in the soil is above a certain critical value, such soils are called frozen (Frolov 1998; Tsytovich 1975). Therefore, dielectric models for describing soils in the region of negative temperatures should describe the processes of the appearance (during cooling) or disappearance (when heated) the ice phase in moist soil samples. Such a spectroscopic dielectric model in the microwave frequency range was proposed by Zhang et al. (2003; 2010), based on the approach proposed by Dobson et al. (1985). As shown in Mironov et al. (2017), this model at a frequency of 1.4 GHz has an unacceptably high statistical error for the CRP values relative to experimental data; specifically, the normalized root-mean-square error (nRMSE) is 26.9% and 85% for the real and imaginary parts of the CRP, respectively. Meanwhile, the development of models CRP of soil at negative temperatures was carried out by other researchers (Mironov and Lukin 2011; Mironov, De Roo, and Savin 2010; Mironov and Savin 2015). In the most complete form, the model was presented in Mironov and Savin (2015). The model is a generalization of previously developed models at positive temperatures (Mironov, Kosolapova, and Fomin 2009; Mironov and Fomin 2009a, 2009b; Mironov, Bobrov, and Fomin 2013a, 2013b; Mironov et al. 2013a). In these models, the ice content was introduced, and was calculated by introducing the temperature dependence of the content of unfrozen water determined from the dielectric measurements of moist soils (Mironov et al. 2018). As a result, TD GRMDM was developed, which described the CRP spectra of individual moist soils not only at positive, but also at negative temperatures.

When considering the above described models, we can conclude that the dielectric models for moist soils are constantly being improved. However, in Mialon et al. (2015), it is noted that there is no universal dielectric model to cover all landscapes and climatic conditions. Therefore, a number of new dielectric models are expected to be developed according to specific territories, such as boreal forests, Arctic tundra areas for frozen/thawed conditions of the soil. Other authors also say that the ability to model of complex permittivity of Arctic soil depending on temperature and texture could be of high interest in developing new remote-sensing products for cold regions (Bircher et al. 2016), determining

the thawed and frozen state of the active topsoil (Derksen et al. 2017), retrieval of soil temperature (Muzalevskiy and Ruzicka 2016), snow research (Schwank et al. 2015).

In this regard, in this article, a dielectric model is developed, which is based on the measured dielectric data of Arctic mineral soils with varying textures. Based on the assumption in Mironov et al. (2017) that the dielectric properties of different components of soil water are weakly dependent on soil texture, an attempt was made to find spectroscopic parameters of soil water simultaneously for a set of soils from one region. This approach can significantly reduce the number of parameters having a dependence on the texture (clay content).

In addition, the dielectric model developed in this paper is based on the approaches (Mironov, Kosolapova, and Fomin 2009), which has several advantages and showed smaller errors in remote sensing in the SMOS algorithm (Mialon et al. 2015). Therefore, we can assume that, using the proposed dielectric model, it will be possible to restore the geophysical parameters of wet Arctic soils in the MHz and GHz frequency ranges with acceptable errors (Mialon et al. 2015; Srivastava et al. 2015) compared to other models. An analysis of the proposed dielectric model as applied to a wide range of satellite systems will be investigated in further works.

## 2. Soil samples and measurement procedures

To develop a dielectric model, we measured three mineral soils collected on the Yamal Peninsula, Russia (soils 1, 2, and 3 from Table 2 in Mironov et al. (2017)). The texture of the soil data in terms of clay content ranged from 9.1 to 41.3%. In addition, for separate verification of the developed dielectric model, measurements were made of another mineral soil with clay content of 33.4% (soil 4 from Table 2 in Mironov et al. (2017)). Dielectric measurements of the soil were carried out for the freezing mode in the temperature range from 25 to $-30\,^{\circ}$C and frequency range from 50 MHz to 15 GHz. The gravimetric moisture of the measured samples varied from dry soil to the maximum field capacity.

Mironov et al. (2017, 2013b) described in detail the sample preparation procedure. Soil samples with a given gravimetric moisture were placed in a measuring container made in the form of a coaxial waveguide. The gravimetric moisture of soil samples ($m_g$) was defined as the ratio of the mass of water in the soil ($m_w$) to the mass of dry soil ($m_d$) that is $m_g = m_w/m_d$. Next, the measuring container was connected to an Agilent vector network analyser and the amplitudes and phases of the components of the scattering matrix $S_{11}$ and $S_{12}$ were measured using the method described in Mironov et al. (2010, 2013c). To obtain the CRP spectra of wet soil samples, an algorithm developed in Mironov et al. (2013c) was applied using the measured scattering matrix data $S_{11}$ and $S_{12}$ for the measuring coaxial container. This algorithm provides the real and imaginary parts of the CRP of moist samples with the errors 10% and 30%, respectively, in the frequency range from 45 MHz to 15 GHz

## 3. Concept of a multi relaxation spectroscopic dielectric model

The generalized refractive mixing dielectric model, as formulated by Mironov and Savin (2015), was used in further consideration. The CRP as follows:

$$\varepsilon_s^* = \varepsilon_s' + i\varepsilon_s'', \tag{1}$$

is expressed through the dielectric constant (DC), $\varepsilon'_s$, and loss factor (LF), $\varepsilon''_s$, where the subscript 's' refer to the moist soil, and 'i' is imaginary unit. In the considered model the complex refractive index (CRI),

$$n_s^* = \sqrt{\varepsilon_s^*} = n_s + \mathrm{i}\kappa_s, \tag{2}$$

is used. Here $n_s$ is the refractive index (RI), and $\kappa_s$ is the normalized attenuation coefficient (NAC) of moist soil, and 'i' is imaginary unit. RI and NAC can be calculated via the DC and LF by the following equations:

$$n_s = \frac{1}{\sqrt{2}}\sqrt{\sqrt{\varepsilon_s'^2 + \varepsilon_s''^2} + \varepsilon_s'^2}, \tag{3}$$

$$\kappa_s = \frac{1}{\sqrt{2}}\sqrt{\sqrt{\varepsilon_s'^2 + \varepsilon_s''^2} - \varepsilon_s'^2} \tag{4}$$

The reversed transitions to the DC and LF are as follows:

$$\varepsilon'_s = n_s^2 - \kappa_s^2, \tag{5}$$

$$\varepsilon''_s = 2n_s\kappa_s. \tag{6}$$

The refractive mixing dielectric model describing the dependences of the soil reduced RI $((n_s - 1)/\rho_d)$ and NAC $(\kappa_s/\rho_d)$ on moisture has the following form:

$$\frac{n_s - 1}{\rho_d} = \begin{cases} \frac{n_m - 1}{\rho_m} + \frac{(n_b - 1)}{\rho_b} m_g, & m_g \le m_{g1}, \\ \frac{n_m - 1}{\rho_m} + \frac{(n_b - 1)}{\rho_b} m_{g1} + \frac{(n_{u,i} - 1)}{\rho_{u,i}} (m_g - m_{g1}), & m_g > m_{g1}, \end{cases} \tag{7}$$

$$\frac{\kappa_s}{\rho_d} = \begin{cases} \frac{\kappa_m}{\rho_m} + \frac{\kappa_b}{\rho_b} m_g, & m_g \le m_{g1}, \\ \frac{\kappa_m}{\rho_m} + \frac{\kappa_b}{\rho_b} m_g + \frac{\kappa_{u,i}}{\rho_{u,i}} (m_g - m_{g1}), & m_g > m_{g1}, \end{cases} \tag{8}$$

where $\rho$ is the density and $m_{g1}$ is the maximum content of unfrozen bound water. The subscripts 's, d, m, b, and i' (which are related to $n$, $\kappa$, and $\rho$) refer to the moist soil, dry soil, solid (mineral) component of soil, unfrozen bound water, and moistened ice, respectively. The densities of unfrozen bound water, unbound water and moistened ice are considered the same as for clear water and ice, respectively ($\rho_b = \rho_u = 1$ g cm$^{-3}$ and $\rho_i = 0.917$ g cm$^{-3}$). Equations (7) and (8) explicitly contain the value of the maximum content of unfrozen bound water, and the value of the reduced RI and NAC solid soil component, which can be found by fitting the experimental data for the CRI of the soil using these equations for the specific frequency and temperature. By introducing the parameter $m_{g1}$, it is possible to distinguish two components of soil water in moist soils, namely, bound water and unbound water in thawed soil, as well as bound water and moistened ice in frozen soil, for the moisture ranges $m_g \le m_{g1}$ and $m_g > m_{g1}$, respectively .

Similar to Mironov, Bobrov, and Fomin (2013b) and Mironov and Savin (2015) we express the DC and the LF of the components of soil water in (3, 4) using the equations for the Debye and Maxwell–Wagner multiple relaxations (Kremer and Schonhals 2003; Ahadov 1999) of non-conductive liquids, which account only for bias electric currents:

$$\varepsilon'_p = \frac{\varepsilon_{0pL} - \varepsilon_{0pM}}{1 + (2\pi f\,\tau_{pL})^2} + \frac{\varepsilon_{0pM} - \varepsilon_{0pH}}{1 + (2\pi f\,\tau_{pM})^2} + \frac{\varepsilon_{0pH} - \varepsilon_{\infty pH}}{1 + (2\pi f\,\tau_{pH})^2} + \varepsilon_{\infty pH}, \tag{9}$$

$$\varepsilon''_p = \frac{\varepsilon_{0pL} - \varepsilon_{0pM}}{1 + (2\pi f\,\tau_{pL})^2}(2\pi f\,\tau_{pL}) + \frac{\varepsilon_{0pM} - \varepsilon_{0pH}}{1 + (2\pi f\,\tau_{pM})^2}(2\pi f\,\tau_{pM}) + \frac{\varepsilon_{0pH} - \varepsilon_{\infty pH}}{1 + (2\pi f\,\tau_{pH})^2}(2\pi f\,\tau_{pH}), \tag{10}$$

where $f$ is the frequency; $\varepsilon_{0pL}$, $\varepsilon_{0pM}$, $\varepsilon_{0pH}$ and $\varepsilon_{\infty pH}$ are the low-frequency limits and the high-frequency limit of the real part of the CRP related to the corresponding relaxations. The parameters $\tau_{pL}$, $\tau_{pM}$ and $\tau_{pH}$ are relaxation times. The subscripts 'H, M, and L' refer to the high-, middle-, and low-frequency relaxations, respectively. The subscripts '$p$' refer to each component of soil water ($p$ = b, u and i, which refer to bound water, unbound water and moistened ice, respectively) is described by its own set of relaxation parameters. Later, when experimental data are fitted by Equations (9) and (10) for the studied soils, three relaxation equations will be used for bound water and two for unbound water (having accepted $\varepsilon_{0pL} = \varepsilon_{0pM}$).

The spectroscopic parameters in formulas (9) and (10) can be expressed as a function of temperature. We suggest that the temperature dependences for the low-frequency and high-frequency limits of the DCs ($\varepsilon_{0pL}$, $\varepsilon_{0pM}$, $\varepsilon_{0pH}$ and $\varepsilon_{\infty pH}$) write down follow the equation that was obtained with the use of the Clausius–Mossotti law (Mironov and Savin 2015):

$$\begin{aligned} \varepsilon_{0pQ}(T) &= \frac{1+2\exp(F_{pQ}(T_{s\varepsilon qpQ}) - \beta_{vqpQ}(T - T_{s\varepsilon qpQ}))}{1-\exp(F_{pQ}(T_{s\varepsilon qpQ}) - \beta_{vqpQ}(T - T_{s\varepsilon qpQ}))}, \\ F_{pQ}(T) &= \ln\left[\frac{\varepsilon_{0pQ}(T)-1}{\varepsilon_{0pQ}(T)+1}\right], \end{aligned} \tag{11}$$

where the subscript '$q$' is replaced with 0 and $\infty$ for the low- and high-frequency DC limits, respectively. The subscript '$Q$' represents the low, medium, and high frequencies of relaxation of the water components in the soil, with $Q$ = L, M, H, respectively. $\beta_{vqpQ}$ is the volume expansion coefficient associated with the soil water components, and $T_{s\varepsilon qpQ}$ is the initial temperature, which can be any value from the measured temperature range for the frozen and thawed state. The values of $\beta_{vqpQ}$ and $\varepsilon_{qpQ}(T_{s\varepsilon qpQ})$ can be determined by approximating the experimental data using the theoretical model of (11).

In Mironov and Fomin (2009a) and Mironov and Savin (2015) it was shown that relaxation times ($\tau_{pL}$, $\tau_{pM}$ and $\tau_{pH}$) in the Debye equations (9) and (10) can also be represented as a function on temperature for various components of soil water. We apply this approach and write the temperature dependence of the relaxation time using the Eyring equation (Dorf 1997):

$$\ln\left(\frac{\mathrm{k}T_\mathrm{K}}{\mathrm{h}}\tau_{pQ}\right) = \frac{\Delta H_{pQ}}{\mathrm{R}}\frac{1}{T_\mathrm{K}} - \frac{\Delta S_{pQ}}{\mathrm{R}}, \tag{12}$$

where h is the Plank constant ($6.626 \times 10^{-34}$ Js), k is the Boltzmann constant ($1.38 \times 10^{-23}$ JK$^{-1}$), $\Delta H_{pQ}$ is the activation energy of the relaxation process, R is the universal gas constant ($8.314 \times 10^{3}$ JK$^{-1}$kmol$^{-1}$), $\Delta S_{pQ}$ is the entropy of activation, and $T_\mathrm{K}$ is the temperature in Kelvin. The ratios $\Delta H_{pQ}/\mathrm{R}$ and $\Delta S_{pQ}/\mathrm{R}$, as follow from the expression (12), can be found by linear approximation of the dependences $\ln\left((\mathrm{k}T_\mathrm{K}/\mathrm{h})\tau_{pQ}\right)$ from $1/T_\mathrm{K}$, which were determined from the dielectric measurements. Using the obtained relaxation parameters and solving Equations (5)–(10), we can calculate the DC and LF values of wet soils this only bias currents are taken into account.

The value of DC is determined completely by bias currents and is calculated from Equation (5), in contrast to LF. For LF at low frequencies, it is necessary to consider the contribution of conduction at a constant current. Thus, the LF of moist soils can be expressed as the sum of two conditions: bias currents $\varepsilon''_{sb} = 2n_s\kappa_s$ and conduction currents $\varepsilon''_{sc} = \sigma_s/(2f\varepsilon_r)$. Here $n_s$ and $\kappa_s$ are calculated from Equations (7) and (8), $\sigma_s$ is the specific conductivity of a moist soil, $\varepsilon_r$ is the free space DC equal to 8.854 pF m$^{-1}$. Considering Mironov and Savin (2015), the resulting expression for LF moist soils can be written as follows:

$$\varepsilon''_s = \begin{cases} 2n_s\kappa_s + \rho_d(m_g)\frac{m_g}{\rho_b}\frac{\sigma_b}{2f\varepsilon_r}, & m_g \le m_{g1}, \\ 2n_s\kappa_s + \rho_d(m_g)\frac{\left(\frac{m_{g1}}{\rho_b}\sigma_b + \frac{m_g - m_{g1}}{\rho_{u,i}}\sigma_{u,i}\right)}{2f\varepsilon_r}, & m_g > m_{g1}, \end{cases} \tag{13}$$

where $\sigma_b$, $\sigma_u$, and $\sigma_i$ are the specific conductivities of bound water, unbound water and moistened ice, respectively.

Finally, we suggest that the conductivity, $\sigma_p$, has a linear dependence with temperature, which is characteristic of ionic solutions.

$$\sigma_{pj}(T) = \sigma_{pj}(T_{s\sigma p}) + \beta_{\sigma pj}(T - T_{s\sigma p}), \tag{14}$$

where $\beta_{\sigma pj}$ is the derivative of conductivity with respect to temperature, which is also referred to as the conductivity temperature coefficient, and $\sigma_{pj}(T_{s\sigma p})$ is the value of conductivity at an arbitrary starting temperature, $T_{s\sigma p}$, that is taken from the measured range. Subscript $p$ = b, u and i, which refer to bound water, unbound water and moistened ice, respectively, subscript $j$ refers to the number of soil samples from Table 3 in Mironov et al. (2017). The values of $\sigma_{pj}(T_{s\sigma p})$ and $\beta_{\sigma pj}$ can be determined by fitting the experimental temperature dependences of conductivity, $\sigma_{pj}(T)$, using the theoretical model (14).

The rationale for the application of the spectroscopic dielectric model described above as well as the determination of the corresponding parameters of this model will be described in the next section.

## 4. Dielectric model

### 4.1. Retrieving the parameters of the multi-relaxation spectroscopic dielectric model

As a result of laboratory measurements of three soils, RI and NAC spectra were obtained at different temperatures and frequencies (0.05–15 GHz). Table 3 of Mironov et al. (2017) shows the values of gravimetric moisture and dry density for measured soil samples. These data were used to calculate the reduced RI and NAC, using the refractive dielectric model (7), (8). In Mironov et al. (2018), it was shown that the maximum content of bound water in the soil does not depend on the frequency, and to estimate the values, the averaged frequency values can be used for the reduced RI and NAC. Based on this, Figure 1 shows the values averaged over the frequency of the reduced RI and NAC values for the three soils studied at a temperature of 20 and $-20\,^{\circ}$C depending on the gravimetric moisture.

The symbols show the measured dependencies, and the solid lines show the fitted results using the refraction model of (7) and (8). For the fitting process, the OriginPro application was applied. For data, including measurements of RI and NAC, fitting procedure was applied simultaneously to three soils. Given the assumption by Mironov et al. (2017) that the dielectric properties of water in the soil weakly depend on the clay content, the parameters $(n_m - 1)/\rho_m$, $\kappa_m/\rho_m$, $(n_b - 1)/\rho_b$, $\kappa_b/\rho_b$, $(n_{u,i} - 1)/\rho_{u,i}$, and $\kappa_{u,i}/\rho_{u,i}$ were shared for all soils, while the parameter $m_{g1}$ was found for each individual soil and was equal to $m_{g11}$, $m_{g12}$, $m_{g13}$ for soils 1, 2, and 3 from Table 2 in Mironov et al. (2017), respectively. As a result, we find that the maximum content of bound water depends only on temperature and on the clay content. In Mironov and Savin (2015) and Mironov, De Roo, and Savin (2010), it was shown that the values of reduced RI and NAC, which characterize solid soil particles, weakly depend on temperature; furthermore, from Figure 1 it is clear that these parameters are the same for all soils, that is, they do not depend on the clay content. In this regard, they were averaged, and the following values were obtained $(n_m - 1)/\rho_m = 0.4$, and $\kappa_m/\rho_m = 0$.

Figure 1 shows the results of fitting the experimental data of reduced RI and NAC, using the refractive dielectric model (7) and (8). As can be seen from Figure 1, the values calculated with the use of refractive dielectric model are in a good agreement with experimental data, while the dependences of RI and NAC on gravimetric moisture are piecewise linear functions with two linear sections that transform into each other when the value of gravimetric moisture $m_g$ is equal to the maximum content of bound water $m_{g11}$, $m_{g12}$ and $m_{g13}$ for the studied soils. Moreover, for each section of the piecewise linear function, a specific component of soil water, namely, bound water and unbound water in thawed soil, as well as bound water and moistened ice in frozen soil, can be identified for the moisture ranges $m_g \leq m_{g1}$ and $m_g > m_{g1}$, respectively, as defined in Section 3.

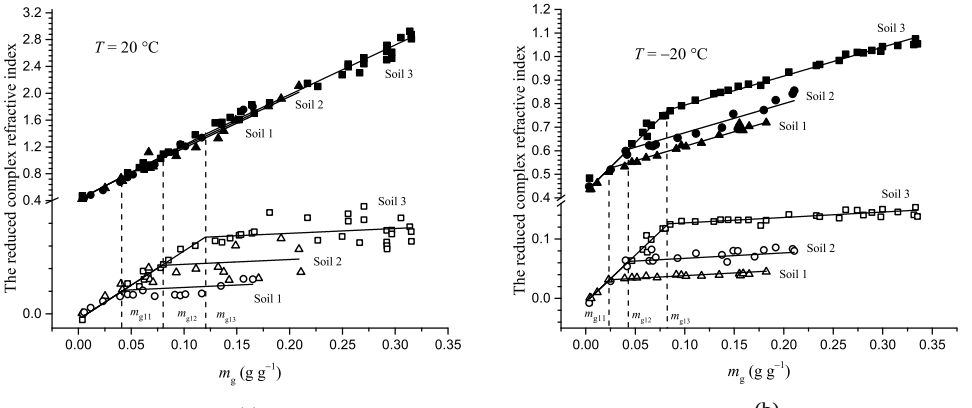


**Figure 1.** The reduced complex refractive index (averaged over the frequency range 0.05–15 GHz) of the measured soils as a function of gravimetric moisture (*a*) at the temperature $T = 20\,^{\circ}\mathrm{C}$, (*b*) at the temperature $T = -20\,^{\circ}\mathrm{C}$. Filled symbols represent reduced RI, $(n_s - 1)/\rho_d$; empty symbols represent NAC, $\kappa_s/\rho_d$.

The parameters $m_{g11}$, $m_{g12}$, and $m_{g13}$ were determined for each measured temperature and are shown by the symbols in Figure 2. For thawed soil the maximum content of bound water does not depend on soil temperature and is determined only by clay content. In describing the temperature dependences of $m_{g1}$ for frozen soil, an exponential function of the following form was used: $m_{g1} = y_0 + A\exp(T/t_0)$. In this function, $T$ is the temperature in °C, $y_0$ is the limiting value of $m_{g1}$ with decreasing temperature, $A$ is maximum change of the value in $m_{g1}$ with decreasing temperature from $T = 0$ °C and $t_0$ is the rate of exponential decrease with decreasing temperature of $m_{g1}$. The fitting was carried out simultaneously for the three studied soils. In the result of applying the regression analysis to the measured data of the maximum content of bound water, using the functions described above, we obtain a temperature and texturally dependent formula for $m_{g1}$:

$$m_{g1} = (0.0066 + 0.0016C) + (-0.0071 + 0.0023C)\exp(\frac{T}{6.9}),\ -30 \le T \le -1\,^{\circ}\mathrm{C} \quad (15)$$

$$m_{g1} = 0.0079 + 0.0034C,\ 0 \le T \le 25\,^{\circ}\mathrm{C} \quad (16)$$

where $C$ is the clay content of the soil in %. The dependences of the maximum content of bound water calculated using Equations (15) and (16), for soils with different clay content, as functions of temperature are shown in Figure 2 by solid lines. In Figure 2, it can be seen that the dependencies of $m_{g1}$ differ by positive and negative temperatures. Therefore, we conditionally assume that the soil samples are in a frozen state in the temperature range $-30 \le T \le -1$ °C. It can also be seen from Figure 2 that the calculated dependences describe the experimental data quite well and are within the limits of errors in the determination of this value from the experimental data.

As a result, the refractive dielectric model CRP for frozen and thawed mineral Arctic soils proposed in Section 3 was experimentally confirmed. Now that the difference between the thawed and frozen states, as well as the maximum content of bound

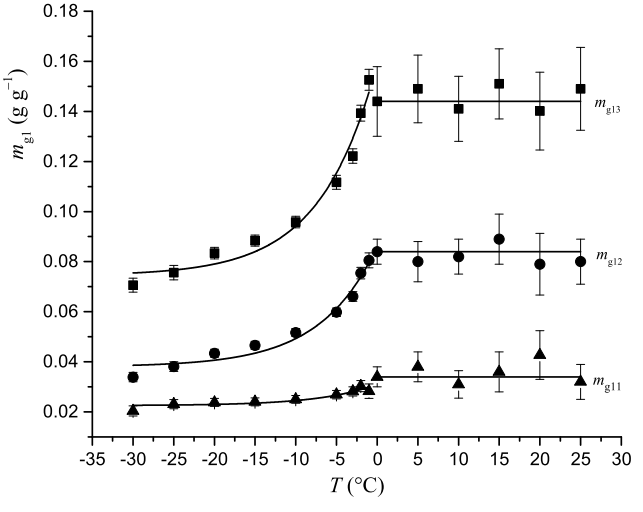


**Figure 2.** The maximum gravimetric content of bound water as a function of temperature. The solid lines indicate the fit results (Equations (16) and (15)).

water, is determined, the next step is to determine the numerical values of the parameters of the spectroscopic dielectric model proposed in Section 3. To solve this problem, we considered the experimental spectra of DC and LF of the studied soils for all measured temperatures and moisture. For example, in Figure 3, the symbols show the experimental DC and LF spectra at a temperature of 20 °C. The search for parameters was carried out in two stages. At the first stage, simultaneous fitting of the DC and LF spectra of the three studied soils was carried out using only measured values of moist soil in the range of $0 < m_g < m_{g1}$, so that only bound water was contained in the samples. As a result, the parameters of the Debye relaxations that relate only to bound water ($\varepsilon_{0bL}$, $\varepsilon_{0bM}$, $\varepsilon_{0bH}$, $\varepsilon_{\infty bH}$, $\tau_{bL}$, $\tau_{bM}$, and $\tau_{bH}$) from Equations (9) and (10) for the frequency range under study was determined. The theoretical model of the soil DC that is fitted to the measured spectra is calculated by applying Equations (3–5), (7–10), and (13). As a result, we obtained, separately for thawed and frozen soils, experimental temperature dependences of the following parameters: the low frequency limit DC ($\varepsilon_{0bL}$ $\varepsilon_{0bM}$, $\varepsilon_{0bH}$), the high frequency limit DC ($\varepsilon_{\infty bH}$), and the corresponding relaxation times ($\tau_{bL}$, $\tau_{bM}$, and $\tau_{bH}$), which were share for all studied soils and refer to the bound water. Besides, we obtained the values of conductivity of bound water, $\sigma_{b1}$, $\sigma_{b2}$, $\sigma_{b3}$, for each soil studied, both in thawed and frozen conditions, where 1, 2, and 3 correspond to the soil number from Table 2 in Mironov et al. (2017). The values of spectroscopic parameters and conductivity, which were determined with an acceptable error for bound water, are shown in Figures 5–7 as a function of temperature.

After all the parameters of the model related to bound water were found, we proceeded to the second stage of fitting. At the next stage, the experimental DC and LF spectra were fitted, and each soil contained both water components, both bound and unbound, that is, the gravimetric moisture of the samples was higher than the maximum content of bound water ($m_g > m_{g1}$). This is necessary to find the parameters for the Debye

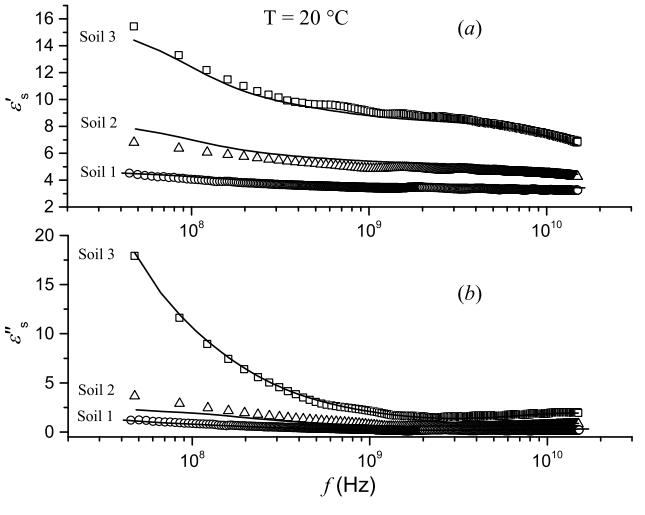


**Figure 3.** Spectra of (a) DC ($\varepsilon'_s$) and (b) LF, $\varepsilon''_s$, for moist soil samples. The measured data are shown by symbols, and the predictions are presented by solid lines. The temperature of soil samples is equal to 20 °C.

relaxation unbound water ($\varepsilon_{0uL}$, $\varepsilon_{0uH}$, $\varepsilon_{\infty uH}$, $\tau_{uL}$ and $\tau_{uH}$) in thawed soil and moistened ice ($\varepsilon_{0iL}$, $\varepsilon_{0iH}$, $\varepsilon_{\infty iH}$, $\tau_{iL}$ and $\tau_{iH}$) in frozen soil, as well as the specific conductivities of unbound water ($\sigma_{u1}$, $\sigma_{u2}$, $\sigma_{u3}$) and moistened ice ($\sigma_{i1}$, $\sigma_{i2}$, $\sigma_{i3}$) in thawed and frozen soil, respectively. To solve this problem, the sequential fitting algorithm described above was used when finding the Debye relaxation parameters in the case when the soil samples contained only bound water. When fitting the measured DC and LF spectra of soil samples containing both bound and unbound water, Equations (3)–(5), (7)–(10), and (13) were used, as well as the previously obtained values ($\varepsilon_{0bL}$, $\varepsilon_{0bM}$, $\varepsilon_{0bH}$, $\varepsilon_{\infty bH}$, $\tau_{bL}$, $\tau_{bM}$, $\tau_{bH}$, $\sigma_{b1}$, $\sigma_{b2}$, and $\sigma_{b3}$) for bound water. As a result, the values of the low frequency limit DC, ($\varepsilon_{0uQ}$), high-frequency limit DC, ($\varepsilon_{\infty uQ}$), relaxation times ($\tau_{uQ}$) and specific conductivities ($\sigma_{uj}(T)$) related to unbound water in the soil were obtained for all measured temperatures. Examples of calculated theoretical DC and LF spectra using the dielectric model and parameters determined from the fit of the measured DC and LF spectra are shown in Figure 4 with solid lines for thawed soil at a temperature of 20 °C and for frozen soil at a temperature of − 20 °C. As can be seen from Figure 4, the spectra calculated using the proposed dielectric model are in a good agreement with experimental data.

The final result presented in this Paragraph are the experimentally obtained temperature dependences of the values of the low-frequency limit DC ($\varepsilon_{0pQ}$), high-frequency limit DC ($\varepsilon_{\infty pQ}$), relaxation times ($\tau_{pQ}$) and also specific conductivities ($\sigma_{pj}(T)$) for bound and unbound water contained in thawed or frozen soil. These dependencies are shown in Figures 5–7. In the next section, the experimental dependencies obtained will be fitted using the Clausius-Mossotti (11) and Eyring (12) equations and the parameters included in these equations are found. As a result, a temperature-dependent multi-relaxation spectroscopic dielectric model for moist mineral soils will be developed.

### 4.2. Parameters of the temperature-dependent dielectric model

A fitting procedure was applied to the experimental temperature dependencies of the low-frequency and high-frequency limits of the DC, the result is shown in Figure 5 ($\varepsilon_{0pL}$,

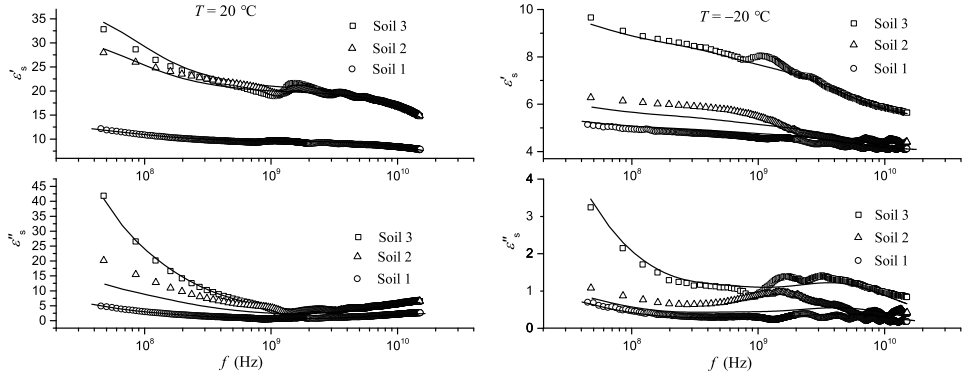


Figure 4. Spectra of (a), (c) DC ($\varepsilon_s'$) and (b), (d) LF ($\varepsilon_s''$) corresponding to the measured data (symbols) and the predictions are presented by solid lines. Moisture of samples are equal to 0.117, 0.191, 0.226 for samples of soils 1, 2 and 3 in (a) and (b), respectively, and 0.135, 0.179, 0.229 for samples 1, 2 and 3 in (c) and (d), respectively.

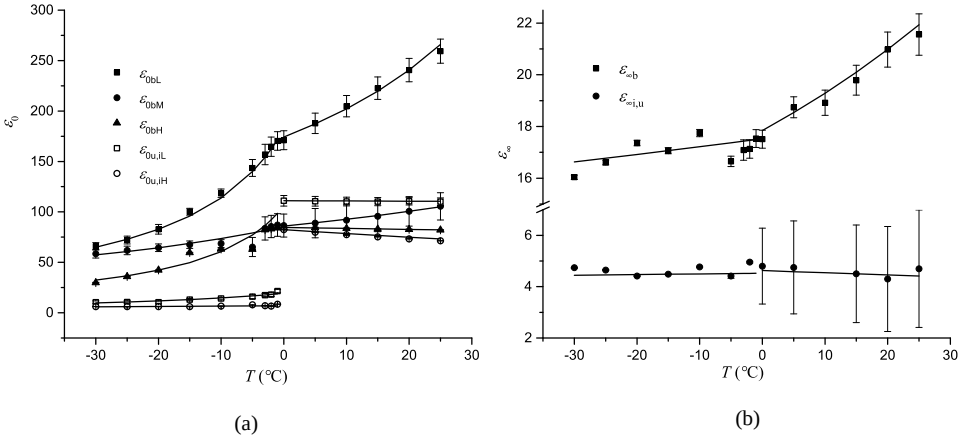


**Figure 5.** (a) Low-frequency limit and (b) high-frequency limits of the DCs as a function of temperature. The measured data and respective fits are shown with symbols and lines, respectively.

$\varepsilon_{0pM}$, $\varepsilon_{0pH}$ and $\varepsilon_{\infty pH}$) using the Clausius–Mossotti equation (11) introduced in Section 2. As a result of this fitting, the parameters of the temperature-dependent dielectric model were determined, namely, the values of the volume expansion coefficient $\beta_{vqpQ}$, as well as the low- and high-frequency limits of the DC at the starting temperature $\varepsilon_{qpQ}(T_{s\varepsilon qpQ})$. The obtained values of the parameters of the temperature-dependent dielectric model, $\beta_{vqpQ}$, $T_{s\varepsilon qpQ}$ and $\varepsilon_{qpQ}(T_{s\varepsilon qpQ})$, were determined separately for thawed and frozen soil samples. These values are shown in Table 1.

In the same way, we fit the experimental temperature dependences of the relaxation times shown in Figure 6, for the various components of water in the soil ($\tau_{pL}$, $\tau_{pM}$, $\tau_{pH}$) using the Eyring Equation (12) given in Section 2. As a result of this fitting, the parameters of the temperature-dependent dielectric model were determined, namely, the values proportional to the activation energy and activation entropy. The obtained values of the parameters of the temperature-dependent dielectric model $\Delta H_{pQ}/\mathrm{R}$ and $\Delta S_{pQ}/\mathrm{R}$ were determined separately for thawed and frozen soil samples. The values of these parameters and their errors are enumerated in Table 1. In addition, by using model (12) and the parameters $\Delta H_{pQ}/\mathrm{R}$ and $\Delta S_{pQ}/\mathrm{R}$, the theoretical values of the relaxation times were calculated. As can be seen from Figure 6 and the errors obtained, the calculated values shown by solid lines describe the measured data well.

Finally, the fit of the temperature dependences of the conductivity shown by the symbols in Figure 7 for individual soils and for the components of the soil water was carried out using the linear dependence (14). As a result of linear fitting, the conductivity value at the starting temperature and the conductivity temperature coefficient were obtained. These values of the parameters of the temperature-dependent dielectric model $\sigma_{pj}(T_{s\sigma p})$ and $\beta_{\sigma pj}$ are determined for thawed and frozen soils separately. It was found that these parameters depend on the clay content. To determine the parameters $\sigma_{pj}(T_{s\sigma p})$ and $\beta_{\sigma pj}$, with respect to clay content, linear approximation was applied, from which the following formulas were obtained:

**Table 1.** The universal parameters of the temperature-dependent dielectric model for all components of soil water in the temperature range $-30\,^{\circ}\mathrm{C} \leq T \leq 25\,^{\circ}\mathrm{C}$.

| | $T \geq 0\,^{\circ}\mathrm{C}$ | | | | |
|---|---|---|---|---|---|
| Soil water component | Bound water ($p$ = b) | | | Unbound water ($p$ = u) | |
| Relaxations | High ($Q$ = H) | Middle ($Q$ = M) | Low ($Q$ = L) | High ($Q$ = H) | Low ($Q$ = L) |
| Parameters | | | | | |
| $\varepsilon_{0p}(T_{s\varepsilon 0pQ})$ | $82.62 \pm 0.363$ | $100.55 \pm 14.671$ | $240.61 \pm 11.608$ | $73.29 \pm 0.228$ | $110.62 \pm 3.734$ |
| $T_{s\varepsilon 0pQ}$ (°C) | | | 20 | | |
| $\beta_{v0pQ}$ ($K^{-1} \times 10^{-3}$) | $0.04 \pm 0.005$ | $-0.25 \pm 0.01$ | $-0.23 \pm 0.01$ | $0.18 \pm 0.013$ | $0.01 \pm 0.003$ |
| $\Delta H_{pQ}/R$ (K) | $1758.89 \pm 28.97$ | $-274.09 \pm 192.64$ | $-338.65 \pm 20.84$ | $2447.41 \pm 171.36$ | $415.87 \pm 42.43$ |
| $\Delta S_{pQ}/R$ | $1.64 \pm 0.11$ | $-8.65 \pm 0.69$ | $-10.46 \pm 0.08$ | $4.49 \pm 0.63$ | $-9.02 \pm 0.15$ |
| $\varepsilon_{\infty p}(T_{s\varepsilon\infty pQ})$ | | $20.98 \pm 0.68$ | | $4.31 \pm 2.70$ | |
| $T_{s\varepsilon\infty pQ}$ (°C) | | | 20 | | |
| $\beta_{v\infty pQ}$ ($K^{-1} \times 10^{-3}$) | | $-1.1 \pm 1.2$ | | $-0.12 \pm 0.14$ | |
| | $T < 0\,^{\circ}\mathrm{C}$ | | | | |
| Soil water component | Unfrozen bound water ($p$ = b) | | | Ice water ($p$ = i) | |
| $\varepsilon_{0p}(T_{s\varepsilon 0pQ})$ | $42.25 \pm 0.337$ | $64.48 \pm 3.731$ | $82.73 \pm 4.804$ | $6.12 \pm 0.048$ | $10.55 \pm 1.207$ |
| $T_{s\varepsilon 0pQ}$ (°C) | | | $-20$ | | |
| $\beta_{v0pQ}$ ($K^{-1} \times 10^{-3}$) | $-2.1 \pm 0.12$ | $-0.57 \pm 0.05$ | $-0.98 \pm 0.02$ | $-2.30 \pm 1.3$ | $-4.70 \pm 0.50$ |
| $\Delta H_{pQ}/R$ (K) | $1530.89 \pm 165.36$ | $-217.89 \pm 184.76$ | $-61.35 \pm 13.02$ | $3456.4 \pm 673.4$ | $93.22 \pm 85.11$ |
| $\Delta S_{pQ}/R$ | $0.72 \pm 0.66$ | $-8.28 \pm 0.73$ | $-9.45 \pm 0.49$ | $8.39 \pm 2.86$ | $-10.23 \pm 0.73$ |
| $\varepsilon_{\infty p}(T_{s\varepsilon\infty pQ})$ | | $17.36 \pm 0.11$ | | $4.42 \pm 0.03$ | |
| $T_{s\varepsilon\infty pQ}$ (°C) | | | $-20$ | | |
| $\beta_{v\infty pQ}$ ($K^{-1} \times 10^{-3}$) | | $-0.29 \pm 0.15$ | | $-0.34 \pm 0.3$ | |

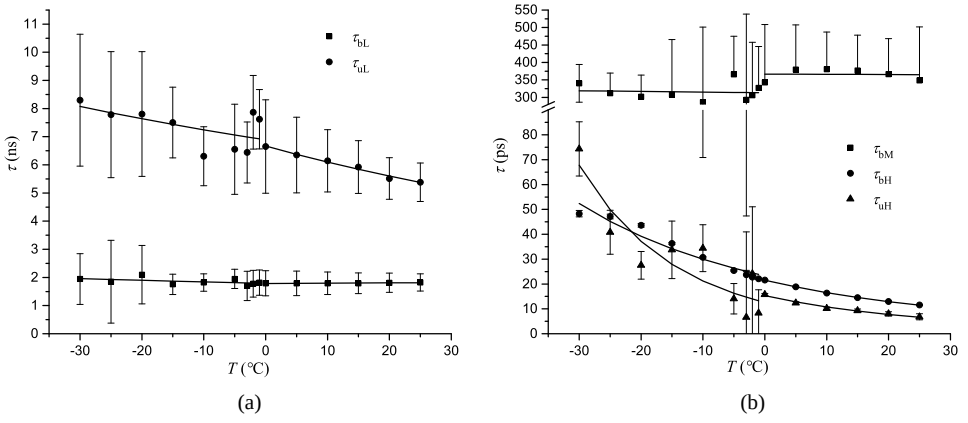


**Figure 6.** Relaxation time as a function of temperature. The measured data and respective fits are shown with symbols and lines, respectively.

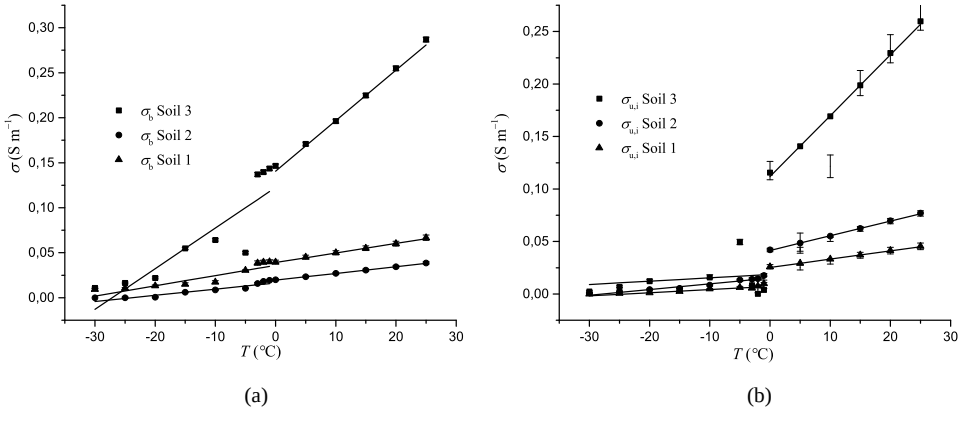


**Figure 7.** Conductivity as a function of temperature. Symbols are data obtained from measurements, lines are the corresponding fitting for bound water (a), free water and moistened ice (b) for all the studied soils.

for the soil in thawed state ($T \geq 0\,^{\circ}\mathrm{C}$)

$$\begin{aligned}
\sigma_{bj}(T_{s\sigma b}) &= (5.8C - 32.9)10^{-3}, \mathrm{S\,m^{-1}},\\
\sigma_{uj}(T_{s\sigma b}) &= (5.2C - 23.8)10^{-3}, \mathrm{S\,m^{-1}},\\
\beta_{\sigma bj} &= (0.15C - 1.1)10^{-3}, (\mathrm{S\,m^{-1}})\,\mathrm{K^{-1}},\\
\beta_{\sigma uj} &= (0.16C - 1.2)10^{-3}, (\mathrm{S\,m^{-1}})\,\mathrm{K^{-1}},
\end{aligned} \tag{17}$$

for the soil in frozen state ($T < 0\,^{\circ}\mathrm{C}$)

$$\begin{aligned}
\sigma_{bj}(T_{s\sigma b}) &= (1.4C - 8.9)10^{-3}, \mathrm{S\,m^{-1}},\\
\sigma_{ij}(T_{s\sigma b}) &= (0.35C - 2.3)10^{-3}, \mathrm{S\,m^{-1}},\\
\beta_{\sigma bj} &= (0.11C - 0.59)10^{-3}, (\mathrm{S\,m^{-1}})\,\mathrm{K^{-1}},\\
\beta_{\sigma ij} &= (-0.00092C + 0.41)10^{-3}, (\mathrm{S\,m^{-1}})\,\mathrm{K^{-1}},
\end{aligned} \tag{18}$$

where $C$ is the clay content of the soil in %.

Using Equations (17) and (18), as well as formula (14), a theoretical model was calculated for the specific conductivity of the various components of water in the soil, which are shown in Figure 7 by solid lines, and good correlation with the experimental data is observed.

### 4.3. Variables and parameters of the dielectric model

As follows from the above analysis, the variables of the model developed for calculating the CRP of a moist soil are the gravimetric moisture, dry soil density electromagnetic wave frequency, soil temperature, and clay content. All these variables are explicitly included in the formulas and relations obtained for the model. In addition, the obtained formulas and relations include groups of universal parameters that retain their values in the entire range of variations of model variables ($m_g$, $\rho_d$, $f$, $T$, $C$) for thawed and frozen soil. These parameters include the reduced RI of the solid soil component ($(n_m - 1)/\rho_m$); reduced NAC of the solid soil component ($\kappa_m/\rho_m$); DC low-frequency limit at the starting temperature for bound water ($\varepsilon_{0bL}(T_{s\varepsilon 0bL})$, $\varepsilon_{0bM}(T_{s\varepsilon 0bM})$, $\varepsilon_{0bH}(T_{s\varepsilon 0bH})$) in the case of thawed and frozen soil, for unbound water ($\varepsilon_{0uL}(T_{s\varepsilon 0uL})$, $\varepsilon_{0uH}(T_{s\varepsilon 0uH})$) in the case of thawed soil and moistened ice ($\varepsilon_{0iL}(T_{s\varepsilon 0iL})$, $\varepsilon_{0iH}(T_{s\varepsilon 0iH})$) in the case of frozen soil; the volume expansion coefficient associated with the low-frequency limit of DC for bound water ($\beta_{v0bL}$, $\beta_{v0bM}$, $\beta_{v0bH}$) in the case of thawed and frozen soil, for unbound water ($\beta_{v0uL}$, $\beta_{v0uH}$) in the case of thawed soil and moistened ice ($\beta_{v0iL}$, $\beta_{v0iH}$) in the case of frozen soil; the parameters of proportional activation entropy for bound water ($\Delta S_{bL}/R$, $\Delta S_{bM}/R$, $\Delta S_{bH}/R$) in the case of thawed and frozen soil, for unbound water ($\Delta S_{uL}/R$, $\Delta S_{uH}/R$) in the case of thawed soil and for moistened ice ($\Delta S_{iL}/R$, $\Delta S_{iH}/R$) in the case of frozen soil; high-frequency DC limit at the starting temperature $\varepsilon_{\infty b}(T_{s\varepsilon\infty bH})$ in the case of thawed and frozen soil, $\varepsilon_{\infty u}(T_{s\varepsilon\infty uH})$ in the case of thawed soil, $\varepsilon_{\infty i}(T_{s\varepsilon\infty iH})$ in the case of frozen soil; and the volume expansion coefficient associated with high-frequency DC limit ($\beta_{v\infty bH}$ when thawed and frozen soil, $\beta_{v\infty uH}$ when thawed soil, $\beta_{v\infty iH}$ in the case of frozen soil). The found numerical values of the universal parameters and the errors with which they are determined are listed in Table 1. The second group includes the parameters of the developed dielectric model, the values of which change with variations in temperature and clay content. These parameters are: the maximum content of unfrozen bound water $m_{g1}$, which is determined from Equations (15) and (16) for thawed and frozen soil cases, respectively; the value of conductivity at the starting temperature $T_{s\sigma p}$, ($\sigma_{bj}(T_{s\sigma b})$), which is determined by Equations (17) and (18) in the case of thawed and frozen soil, respectively; $\sigma_{uj}(T_{s\sigma u})$, which is determined using Equation (17) in the case of thawed soil, $\sigma_{ij}(T_{s\sigma i})$, which is determined using Equation (18) in the case of frozen soil, and the thermal conductivity coefficient ($\beta_{\sigma bj}$, which is determined using Equations (17) and (18) in the case of thawed and frozen soil, respectively; $\beta_{\sigma uj}$, which is determined using Equation (17) in the case of thawed soil, and $\beta_{\sigma ij}$, which is determined using Equation (18) in the case of frozen soil).

The algorithm, based on the above formulas, ratios and parameters, that calculates the values of DC and LF of soil has the following form:

(1) Set the model variables ($m_g$, $\rho_d$, $f$, $T$, $C$).

(2) The high-frequency and low-frequency limits of the DC, as well as relaxation times, are calculated using Equation (11), (12) and the data given in Table 1 at a given temperature.

(3) After the values of $\varepsilon_{qpQ}$ and $\tau_{pQ}$ are found, the values of DC, $\varepsilon'_p$, and LF, $\varepsilon''_p$, for all water components in the soil are calculated as functions of frequency at a given temperature using the Debye multi-relaxation Equations (9) and (10), respectively.

(4) The values of $\varepsilon'_p$ and $\varepsilon''_p$ are translated into RI and NAC for all components of the soil water using Equations (3) and (4).

(5) Using the refraction models (7) and (8), and Equations (15) and (16) for the maximum content of bound water, as well as the values of the parameters $(n_m - 1)/\rho_m = 0.4$ and $\kappa_m/\rho_m = 0$ for given values the variables $m_g$ and $\rho_d$ are calculated by RI and NAC by soils.

(6) Finally, the values of RI and NAC of soil are converted to DC and LF soil, using Equations (5) and (13), respectively, accounting for the conductivity, which is calculated using Equations (14), (17) and (18).

In the next section, we will evaluate the developed dielectric model by comparing the calculated values of DC and LF with the corresponding measured data. In addition, a comparative analysis will be made of the $\varepsilon'_s$ and $\varepsilon''_s$ values calculated using the dielectric model proposed in this article with measured data that were not used in developing the model to verify the applicability of the proposed model for separate soil .

## 5. Validation of the developed dielectric model

To quantify the statistical error of the proposed dielectric model, we estimated the value of determination coefficient ($R^2$) and the value of the nRMSE for the calculated values of DC and LF relative to the measured data, the values of which were used for creating a model. The formulas given in Section 4 of Mironov et al. (2017) were used. The

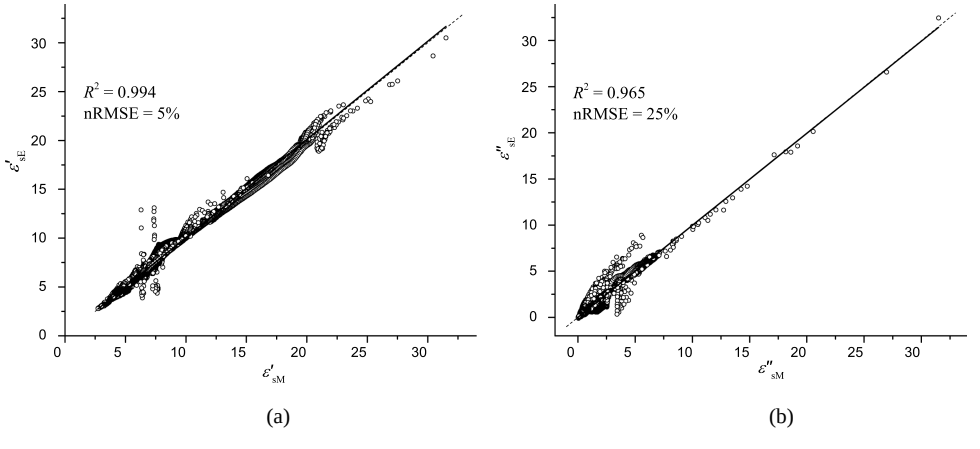


**Figure 8.** The predicted CRP of moist soil as a function of the measured one in the temperature ranges of $-30\,^{\circ}\mathrm{C} \le T \le 25\,^{\circ}\mathrm{C}$. (a) the DC, $\varepsilon'_s$, (b) the LF, $\varepsilon''_s$. The bisectors are denoted by dashed lines.

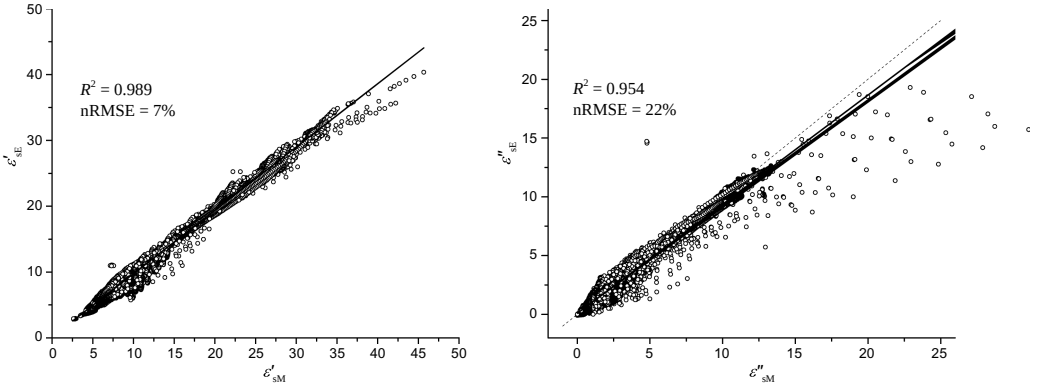


**Figure 9.** The predicted CRP of separate moist soil as a function of the measured one in the temperature ranges of $-30\,^{\circ}\mathrm{C} \leq T \leq 25\,^{\circ}\mathrm{C}$. (a) The DC, $\varepsilon'_s$, (b) the LF, $\varepsilon''_s$. The bisectors are denoted by dashed lines.

correspondence between the calculated values of DC and LF and the measured values is shown in Figure 8. As a result, nRMSE $= 5\%$ for DC, and nRMSE $= 25\%$ for LF of the moist soils were obtained. The values of $R^2$ were equal to 0.994 and 0.965 for DC and LF, respectively. From the obtained results it is clear that the errors of the developed model are close to the measurement errors of the corresponding values (see Section 2).

In addition, to assess the applicability of the developed dielectric model for separate soil, the same estimation was carried out as suggested above for the additionally measured Arctic soil with a clay content of $33.4\%$ (soil 4 from Table 2 in Mironov et al. (2017)). The measured dielectric data of this soil was not used in the model development. To calculate the theoretical CRP spectra of a separate soil, the above described method and spectroscopic parameters are used, as listed in Table 1. The correspondence between the calculated values of DC and LF and the measured values is shown in Figure 9. As a result, nRMSE values of $7\%$ and $22\%$ were obtained, and the $R^2$ values were found to be 0.989 and 0.954 for DC and LF, respectively. As a result, it was shown that for the separate soils, close error values were obtained as in the case of these soils, the dielectric data were used in the model development.

## 6. Conclusions

Based on measurements of three mineral soils collected in the Arctic tundra at the Yamal Peninsula site, a spectroscopic (frequency range 0.05–15 GHz) dielectric model for both the thawed and frozen state was developed. The developed model accounts for the dependence of CRP on moisture (in the range of gravimetric moisture values from 0 to 0.32 $\mathrm{g\,g^{-1}}$), dry soil density (from 1.28 to 1.86 $\mathrm{g\,cm^{-3}}$), and clay content (from 9.1 to $41.3\%$) for temperatures in the range from $-30$ to $25\,^{\circ}\mathrm{C}$. In contrast with previous dielectric models, a new approach was proposed to derive the universal parameters of the proposed dielectric model, which ensures simultaneous fitting of the DC and LF spectra for all soils with different textures belonging to the group of soils under

consideration. This approach also provides the error estimations for the obtained parameters of the developed dielectric model.

The developed model allows to predict the CRP values that correspond well with the dielectric measurements. In particular, this correspondence is characterized by the values of $R^2$ which is equal to 0.994 and 0.965 for DC and LF, respectively. The value of the nRMSE for the real and imaginary parts of the CRP is 5% and 25%, respectively. The errors of these CRP predictions calculated with the use of the proposed dielectric model have the same order of values as the dielectric measurement errors themselves. In addition, to assess the applicability of the developed dielectric model for separate soil, the same estimation was carried out as suggested above, using data from the additionally measured Arctic soil, which was not used in the development of the model. As a result, nRMSE values of 7% and 22% were obtained, and the $R^2$ values were found to be 0.989 and 0.954 for DC and LF, respectively.

Future, studies can involve testing the proposed dielectric model for the measured soil data from other regions.

## References


Ahadov, Y. Y. 1999. "Dielectrical Parametrs of Pure Liquids." MAI M. doi:10.1046/j.1469-1809.1999.6320101.x.

Bindlish, R., M. H. Cosh, T. J. Jackson, T. Koike, H. Fujii, S. K. Chan, J. Asanuma, et al. 2017. "GCOM-W AMSR2 Soil Moisture Product Validation Using Core Validation Sites." *IEEE Journal of Selected Topics in Applied Earth Observations and Remote Sensing* 11 (1): 209–219. doi:10.1109/JSTARS.2017.2754293.

Birchak, J. R., C. G. Gardner, J. E. Hipp, and J. M. Victor. 1974. "High Dielectric Constant Microwave Probes for Sensing Soil Moisture." *Proceedings of the IEEE* 62 (1): 93–98. doi:10.1109/PROC.1974.9388.

Bircher, S., F. Demontoux, S. Razafindratsima, E. Zakharova, M. Drusch, J.-P. Wigneron, and Y. Kerr. 2016. "L-band Relative Permittivity of Organic Soil Surface layers–A New Dataset of Resonant Cavity Measurements and Model Evaluation." *Remote Sensing* 8 (12): 1024. doi:10.3390/rs8121024.

Curtis, J. O., C. A. Weiss, and J. B. Everett. 1995. "Effect of Soil Composition on Dielectric Properties." US Army Corps Eng. Waterways Exp. Station, Vicksburg, MS, Tech. Rep. EL-95-34.

Derksen, C., X. Xiaolan, R. Scott Dunbar, A. Colliander, Y. Kim, J. S. Kimball, T. Andrew Black, et al. 2017. "Retrieving Landscape Freeze/thaw State from Soil Moisture Active Passive (SMAP) Radar and Radiometer Measurements". *Remote Sensing of Environment* 194: 48–62. doi:10.1016/j.rse.2017.03.007.

Dobson, M. C., F. T. Ulaby, M. T. Hallikainen, and M. A. El-rayes. 1985. "Microwave Dielectric Behavior of Wet Soil-Part II: Dielectric Mixing Models." *IEEE Transactions on Geoscience and Remote Sensing* GE-23 (1): 35–46. doi:10.1109/TGRS.1985.289498.

Dorf, R. C. 1997. *The Electrical Engineering Handbook*. 2nd ed. Electrical Engineering Handbook. CRC press. https://books.google.ru/books?id=qP7HvuakLgEC.

Frolov, A. D. 1998. *Electric and Elastic Properties of Frozen Earth Materials*. Pushchino: ONTI PNC Russian Academy of Science Press.

Jackson, T. J., M. H. Cosh, R. Bindlish, P. J. Starks, D. D. Bosch, M. Seyfried, D. C. Goodrich, M. S. Moran, and D. Jinyang. 2010. "Validation of Advanced Microwave Scanning Radiometer Soil Moisture Products." *IEEE Transactions on Geoscience and Remote Sensing* 48 (12): 4256–4272. doi:10.1109/TGRS.2010.2051035.

Kremer, F., and A. Schonhals. 2003. *Broadband Dielectric Spectroscopy*. Berlin, Heidelberg: Springer.

Mialon, A., P. Richaume, D. Leroux, S. Bircher, A. A. Bitar, T. Pellarin, J. Wigneron, and Y. H. Kerr. 2015. "Comparison of Dobson and Mironov Dielectric Models in the SMOS Soil Moisture Retrieval Algorithm." *IEEE Transactions on Geoscience and Remote Sensing* 53 (6): 3084–3094. doi:10.1109/TGRS.2014.2368585.

Mironov, V., and S. Fomin. 2009a. "Temperature Dependable Microwave Dielectric Model for Moist Soils." *Proceedings PIERS* 1: 831–835.

Mironov, V. L., L. G. Kosolapova, Y. I. Lukin, A. Y. Karavaysky, and I. P. Molostov. 2017. "Temperature- and Texture-dependent Dielectric Model for Frozen and Thawed Mineral Soils at a Frequency of 1.4 GHz." *Remote Sensing of Environment* 200: 240–249. doi:10.1016/j.rse.2017.08.007.

Mironov, V. L., P. P. Bobrov, and S. V. Fomin. 2013a. "Dielectric Model of Moist Soils with Varying Clay Content in the 0.04 To 26.5 GHz Frequency Range." In *2013 International Siberian Conference on Control and Communications (SIBCON)*, Krasnoyarsk, Sep., 1–4.

Mironov, V. L., P. P. Bobrov, and S. V. Fomin. 2013b. "Multirelaxation Generalized Refractive Mixing Dielectric Model of Moist Soils." *IEEE Geoscience and Remote Sensing Letters* 10 (3): 603–606. doi:10.1109/LGRS.2012.2215574.

Mironov, V. L., P. P. Bobrov, S. V. Fomin, and A. Y. Karavaiskii. 2013a. "Generalized Refractive Mixing Dielectric Model of Moist Soils considering Ionic Relaxation of Soil Water." *Russian Physics Journal* 56 (3): 319–324. doi:10.1007/s11182-013-0034-4.

Mironov, V. L., R. D. De Roo, and I. V. Savin. 2010. "Temperature-Dependable Microwave Dielectric Model for an Arctic Soil." *IEEE Transactions on Geoscience and Remote Sensing* 48 (6): 2544–2556. doi:10.1109/TGRS.2010.2040034.

Mironov, V. L., M. C. Dobson, V. H. Kaupp, S. A. Komarov, and V. N. Kleshchenko. 2004. "Generalized Refractive Mixing Dielectric Model for Moist Soils." *IEEE Transactions on Geoscience and Remote Sensing* 42 (4): 773–785. doi:10.1109/TGRS.2003.823288.

Mironov, V. L., and S. V. Fomin. 2009b. "Temperature and Mineralogy Dependable Model for Microwave Dielectric Spectra of Moist Soils." *Piers Online* 5: 411–415. doi:10.2529/PIERS090220054025.

Mironov, V. L., A. Y. Karavayskiy, Y. I. Lukin, and E. I. Pogoreltsev. 2018. "Joint Studies of Water Phase Transitions in Na-bentonite Clay by Calorimetric and Dielectric Methods." *Cold Regions Science and Technology* 153: 172–180. doi:10.1016/j.coldregions.2018.04.010.

Mironov, V. L., Y. Kerr, J.-P. Wigneron, L. Kosolapova, and F. Demontoux. 2013b. "Temperature- and Texture-Dependent Dielectric Model for Moist Soils at 1.4 GHz." *Geoscience and Remote Sensing Letters, IEEE* 10: 419–423. doi:10.1109/LGRS.2012.2207878.

Mironov, V. L., S. A. Komarov, Y. I. Lukin, and D. S. Shatov. 2010. "A Technique for Measuring the Frequency Spectrum of the Complex Permittivity of Soil." *Journal of Communications Technology and Electronics* 55 (12): 1368–1373. doi:10.1134/S1064226910120065.

Mironov, V. L., L. G. Kosolapova, and S. V. Fomin. 2009. "Physically and Mineralogically Based Spectroscopic Dielectric Model for Moist Soils." *IEEE Transactions on Geoscience and Remote Sensing* 47 (7): 2059–2070. doi:10.1109/TGRS.2008.2011631.

Mironov, V. L., and Y. I. Lukin. 2011. "A Physical Model of Dielectric Spectra of Thawed and Frozen Bentonitic Clay within the Frequency Range from 1 to 15 GHz." *Russian Physics Journal* 53 (9): 956–963. doi:10.1007/s11182-011-9516-4.

Mironov, V. L., I. P. Molostov, Y. I. Lukin, and A. Y. Karavaisky. 2013c. "Method of Retrieving Permittivity from $S_{12}$ Element of the Waveguide Scattering Matrix." In *2013 International Siberian Conference on Control and Communications (SIBCON)*, Krasnoyarsk, 1–3.

Mironov, V. L., and I. V. Savin. 2015. "A Temperature-dependent Multi-relaxation Spectroscopic Dielectric Model for Thawed and Frozen Organic Soil at 0.05 – 15 GHz." *Physics and Chemistry of the Earth, Parts A/B/C* 83-84: 57–64. Emerging science and applications with microwave remote sensing data http://www.sciencedirect.com/science/article/pii/S1474706515000224

Muzalevskiy, K. V., and Z. Ruzicka. 2016. "Retrieving Soil Temperature at a Test Site on the Yamal Peninsula Based on the SMOS Brightness Temperature Observations." *IEEE Journal of Selected Topics in Applied Earth Observations and Remote Sensing* 9 (6): 2468–2477. doi:10.1109/JSTARS.2016.2553220.

Peplinski, N. R., F. T. Ulaby, and M. C. Dobson. 1995. "Dielectric Properties of Soils in the 0.3–1.3 GHz Range." *IEEE Transactions on Geoscience and Remote Sensing* 33 (3): 803–807. doi:10.1109/36.387598.

Schwank, M., C. Mätzler, A. Wiesmann, U. Wegmüller, J. Pulliainen, J. Lemmetyinen, K. Rautiainen, C. Derksen, P. Toose, and M. Drusch. 2015. "Snow Density and Ground Permittivity Retrieved from L-band Radiometry: A Synthetic Analysis." *IEEE Journal of Selected Topics in Applied Earth Observations and Remote Sensing* 8 (8): 3833–3845. doi:10.1109/JSTARS.4609443.

Srivastava, P. K., P. O'Neill, M. Cosh, M. Kurum, R. Lang, and A. Joseph. 2015. "Evaluation of Dielectric Mixing Models for Passive Microwave Soil Moisture Retrieval Using Data from ComRAD Ground-Based SMAP Simulator." *IEEE Journal of Selected Topics in Applied Earth Observations and Remote Sensing* 8 (9): 4345–4354. doi:10.1109/JSTARS.2014.2372031.

Tabatabaeenejad, A., M. Burgin, X. Duan, and M. Moghaddam. 2014. "P-band Radar Retrieval of Subsurface Soil Moisture Profile as a Second-order Polynomial: First AirMOSS Results." *IEEE Transactions on Geoscience and Remote Sensing* 53 (2): 645–658. doi:10.1109/TGRS.2014.2326839.

Tsytovich, N. A. 1975. *Mechanics of Frozen Ground*. Moscow: Scripta Book.

Wagner, N., K. Emmerich, F. Bonitz, and K. Kupfer. 2011. "Experimental Investigations on the Frequency- and Temperature-Dependent Dielectric Material Properties of Soil." *IEEE Transactions on Geoscience and Remote Sensing* 49 (7): 2518–2530. doi:10.1109/TGRS.2011.2108303.

Wang, J. R., and T. J. Schmugge. 1980. "An Empirical Model for the Complex Dielectric Permittivity of Soils as a Function of Water Content." *IEEE Transactions on Geoscience and Remote Sensing* GE-18 (4): 288–295. doi:10.1109/TGRS.1980.350304.

Wigneron, J.-P., T. J. Jackson, P. O'Neill, G. De Lannoy, P. Rosnay, J. Walker, P. Ferrazzoli, et al. 2017. "Modelling the Passive Microwave Signature from Land Surfaces: A Review of Recent Results and Application to the L-band SMOS & SMAP Soil Moisture Retrieval Algorithms". *Remote Sensing of Environment* 192: 238–262. doi:10.1016/j.rse.2017.01.024.

Zeng, J., K.-S. Chen, B. Haiyun, and Q. Chen. 2016. "A Preliminary Evaluation of the SMAP Radiometer Soil Moisture Product over United States and Europe Using Ground-based Measurements." *IEEE Transactions on Geoscience and Remote Sensing* 54 (8): 4929–4940. doi:10.1109/TGRS.2016.2553085.

Zhang, L., T. Zhao, L. Jiang, and S. Zhao. 2010. "Estimate of Phase Transition Water Content in Freeze–Thaw Process Using Microwave Radiometer." *IEEE Transactions on Geoscience and Remote Sensing* 48 (12): 4248–4255. doi:10.1109/TGRS.2010.2051158.

Zhang, L., J. Shi, Z. Zhang, and K. Zhao. 2003. "The Estimation of Dielectric Constant of Frozen Soil-water Mixture at Microwave Bands." In *IGARSS 2003. 2003 IEEE International Geoscience and Remote Sensing Symposium. Proceedings (IEEE Cat. No.03CH37477)*, Vol. 4, Toulouse, France, July, 2903–2905.